Theoretical study on haloaromatic radical anions and their intramolecular electron transfer reactions

Adriana B. Pierini * **and José S. Duca, Jr.**
INFIQC, Departamento de Química Orgánica, Facultad de Ciencias Químicas, Universidad Nacional de Córdoba, C.C. 61, (5016) Córdoba, Argentina

An AM1 theoretical study was made on the electronic nature of radical anions of halobenzenes, 2-halopyridines, halobenzonitriles, *ortho*-, *para*-, *meta*-haloacetophenones and related compounds ($X = Cl$, Br and I). The experimentally determined fragmentation rate of these intermediates is discussed in terms of the possibility of the existence of π^* and σ^* orbital isomeric radical anions, their energy difference and the probability of an intramolecular electron-transfer reaction from the π^* to the σ^* system. Good correlation was obtained between the properties determined theoretically and the experimental fragmentation rates for the family of halobenzonitrile and haloacetophenone compounds.

Inspection of the potential surface for the intramolecular electron-transfer reaction between both isomers indicates that the carbon–halogen bond elongation and bending angle are the main reaction coordinates for the electron-transfer step which results from an avoided crossing of potential energy surfaces (non-vanishing $H_{\sigma\pi}$ integral).

Radical anions (RAs) of haloaromatic compounds have been proposed as intermediates in different types of reactions,[1] among them nucleophilic substitution processes that take place through electron transfer (ET) steps. The $S_{RN}1$ [2] radical chain mechanism is one of the most common processes by which these nucleophilic substitutions can occur (Scheme 1).

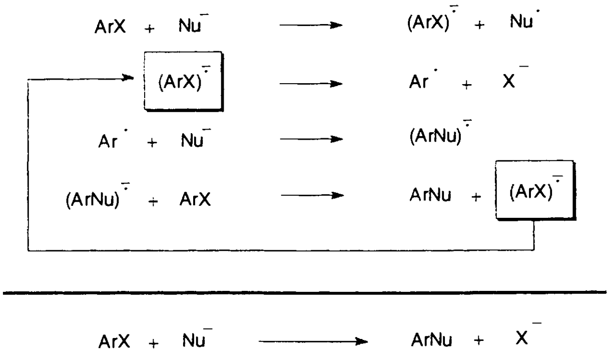

Scheme 1

Formation of the RA of the substrate has been proposed as the initial step. This intermediate has an enhanced reactivity with respect to the parent neutral molecule in the C–halogen (hereafter C–X) bond breaking reaction, as has been recently determined by thermodynamic cycles[3] and *ab initio* calculations.[4] This process has significant importance in the substitution reaction.

For non-strained aliphatic halides the initial ET reaction has been proposed to be dissociative leading directly to the radical and the anion of the leaving group.[2c,5]

Halobenzenes, unactivated aromatic and heteroaromatic halides, electron-withdrawing substituted aliphatic halides, vinyl, bridgehead, neopentyl, cycloalkyl and perfluoroalkyl halides have been extensively studied as substrates of these reactions with a wide variety of nucleophiles.[2,6]

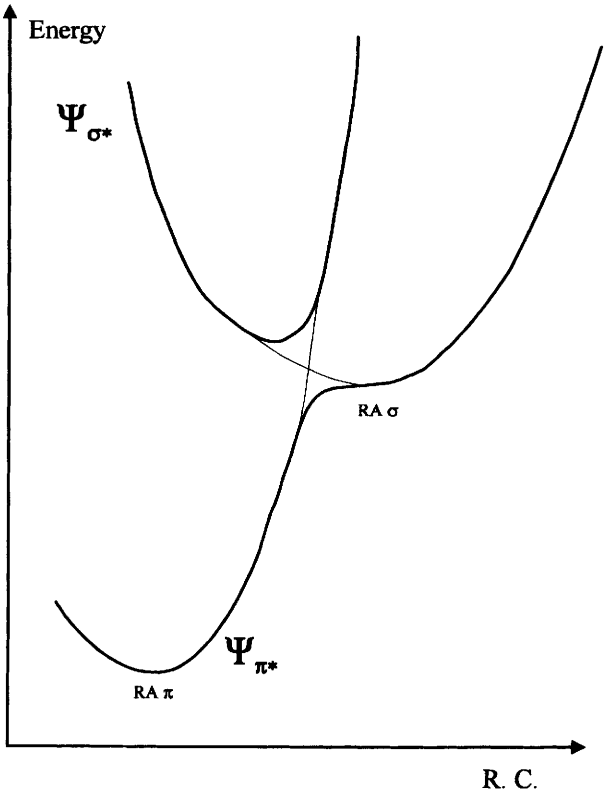

Fig. 1 Potential energy profile for a hypothetical endergonic π–σ isomerism. Dissociation at long C–X distances (R.C.) is not shown.

Aromatic RAs may present π^*–σ^* orbital isomerism depending on the orbital symmetry of the single occupied molecular orbital (SOMO).† This isomerism is possible for those systems in which excitation of the unpaired electron, from a singly occupied to a low lying unoccupied MO of different symmetry, gives rise, after internal coordinates rearrangement, to a species that differs in geometry from the initial state, both species corresponding to different local minima on the ground-state surface.[7] This orbital isomerism [eqn. (1)] is presented in

---

† Orbital isomers are defined as species distinguishable by different occupation of a set of available MOs. The MOs may be distinguished by symmetry, or by their nodal properties. See: M. J. S. Dewar, S. Kirschner and H. W. Kollmar, *J. Am. Chem. Soc.*, 1974, **96**, 5242.

$$\mathrm{ArX} + e^- \longrightarrow \underset{\mathrm{RA}\,\pi}{{}^{\bullet -}(\mathrm{Ar})\text{–}\mathrm{X}} \xrightarrow{\mathrm{IET}} \underset{\mathrm{RA}\,\sigma}{\mathrm{Ar}\overset{-}{\text{–}}\mathrm{X}} \longrightarrow \mathrm{Ar}^{\bullet} + \mathrm{X}^- \quad (1)$$

Fig. 1 for a gas-phase endergonic π*–σ* isomerization reaction which can be viewed as an intramolecular ET process (IET).

From the two possible aromatic RAs, it has been proposed[2a] that the σ* RA (henceforth RA σ and RA π for π* RA) can dissociate in the sense indicated by eqn. (1) to give the corresponding aromatic radical and the anion of the leaving group. According to this, the σ curve of Fig. 1 ends up in the dissociation fragments at long C–X distances. This curve has been proposed as repulsive at all C–X separation distances but infinity.[8] However, RAs σ have been reported as intermediates both theoretically[9] and spectroscopically.[10] The RA σ can cleave through an endergonic or exergonic process. Exergonicity has been proposed for the fragmentation reaction of haloaromatic RAs (*e.g.* PhCl) in the cases in which the electron affinity of the halide leaving atom is higher than the C–X bond dissociation energy.[8]

Based on previous considerations, the fragmentation reaction of halo aromatic RAs can be viewed as an IET step from the π system to the σ C–X bond.[11]

ET reactions have attracted much attention, particularly in relation to indirect donor–acceptor coupling mediated by intervening materials (spacers).[12] Such studies have important targets *e.g.* long-range ET in proteins[13] and controlled ET.[14] In contrast, almost no theoretical studies have been made on the π–σ orbital isomerism of halobenzenes RAs and related compounds,[15] in which no spacer mediates the process. The evaluation of the reaction was only made qualitatively based on empirical rules.[16] Among the studies carried out on the system, extended Hückel[17] and MNDO calculations have been reported.[15,18] The most stable intermediates were located with the MNDO method for the RAs of the compounds C_6H_5X, C_6F_5X (X = Cl, Br or I), *o*-, *m*- and *p*-$C_6H_4X_2$ and $C_6F_4X_2$ (X = Br or I)[18] while the orbital isomerism for halobenzenes RAs has been informed on the basis of the same procedure.[15]

Theoretical calculations on the C–O fragmentation in RAs of phenyl, benzyl and nitrophenyl methyl ethers have also been reported.[19,20]

The present paper involves a theoretical study, carried out with the AM1[21] semi-empirical method, of the potential surface of $(\mathrm{ArX})^{\bullet -}$ in order to determine the feasibility of RA isomerism for halobenzenes, 2-halopyridines (X = Cl, Br, I), a series of halobenzonitriles, *o*-, *m*-, *p*-haloacetophenones and related compounds as well as the nature of the reaction coordinates (C–X bond elongation and C–X bond angle deviation) for the IET process. For those cases where the π–σ RAs were characterized as a minimum of the potential surface, the activation energy of the IET reaction is discussed in terms of the energy difference between both isomers ($\Delta E_{\sigma\pi}$). Correlation of these theoretical values and the experimental fragmentation rates are presented for the haloacetophenone and halobenzonitrile family of compounds.

Computational procedure

All calculations were carried out by the semi-empirical AM1 method as implemented in AMPAC‡,[22] within the UHF formalism in order to account properly for the electronic nature of the species under study.[23]

The equilibrium geometries were obtained with complete geometry optimization without making assumptions. The stationary points were characterized by calculating their Hessian matrix, no negative eigenvalue for a minimum energy structure and one negative eigenvalue for a transition state.[24]

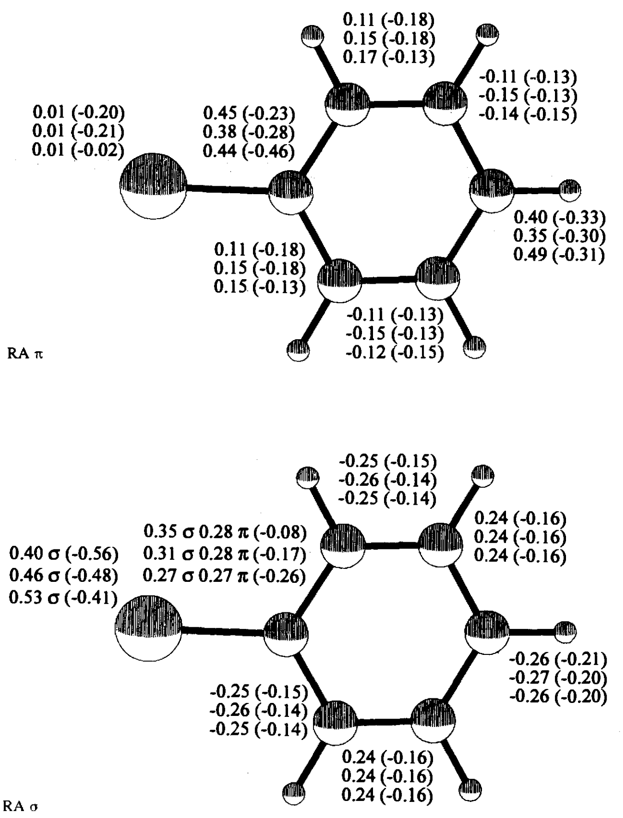

Fig. 2 Charge (in parentheses) and π unpaired spin distribution (otherwise indicated) for the halobenzenes RA π and RA σ. From top to bottom, values for PhX (X = Cl, Br and I) are shown for each atom.

The AM1 UHF procedure usually leads to the most stable RA of each compound. The less stable RA was found by starting with the bond-order matrix of the most stable one, modified by promotion of the unpaired electron to an unoccupied MO of the required symmetry, following the procedure previously described.[7b]

Another approach to obtain the RA σ involves starting the calculation with the geometry of a loose radical–halide ion complex. Both methodologies lead to the same and unique RA σ, located on the ground state potential energy hypersurface.

Once each RA has been located, inspection of the potential energy surface for their interconversion is performed through the reaction coordinate method by small displacements of the C–X bond length and of the dihedral angle formed by the C–X bond and the aromatic ring. During this procedure every other internal coordinate remained practically unchanged.

It is known that the UHF wavefunction is not an eigenfunction of the S^2 operator. For some RAs, a value slightly higher than 0.75 (corresponding to a pure doublet) was obtained as the eigenvalue of this operator, indicating a small degree of spin contamination.

AM1 RHF/CI calculations have also been performed. Thus, keeping $M_s = 1/2$, all single excited configurations arising from an active subspace of one electron and three or four orbitals were included, *i.e.* CI configurations (1,3) and (1,4). Ground state and excited state minima were calculated by RHF/CI with complete geometry optimization.

Results

Halobenzenes and 2-halopyridines

The main geometric parameters and the heats of formation

---

‡ Detailed structures: AMPAC archive files for all the species reported here are available from the authors on an MS-DOS floppy disk.

Table 1 AM1 heats of formation, C–X bond distances and twist angles of π and σ radical anions of halobenzenes and 2-halopyridines

	Δ_fH/kcal mol^{-1}		r(C–X)/Å		C–X dihedral angle[a]/ degrees	
Molecule	RA π	RA σ	RA π	RA σ	RA π	RA σ
Chlorobenzene	5.65	10.91[b] 14.77[c]	1.772	1.956	163.5	148.6[b] 179.9[c]
Bromobenzene	14.32	16.37	1.925	2.064	159.3	178.8
Iodobenzene	24.05	22.86	2.052	2.165	177.6	179.9
2-Chloropyridine	9.00	13.35[b] 18.87[c]	1.746	1.967	164.2	148.0[b] 180.0[c]
2-Bromopyridine	17.59	20.66	1.913	2.070	162.7	179.6
2-Iodopyridine	27.34	26.95	2.025	2.168	176.9	179.1

[a] Angle taken with respect to the aromatic ring. [b] Crossing between the π and σ surfaces (see explanation in the text). [c] Transition state for halogen bending of the σ state (see explanation in the text).

calculated for the halobenzene and 2-halopyridine RAs are shown in Table 1, whereas the unpaired spin and negative charge distribution are presented in Fig. 2 for a group of representative RAs.

The main geometric differences between both isomers are the C–X bond length and the C–X aromatic ring bending angle.§

In the RA π the ring presents a certain degree of bond alternation and a C–X bond distance quite similar to that of the neutral compound. The C–X bond deviates from planarity for X = Cl and Br, while it remains planar for X = I. For iodobenzene the geometric changes produced on the neutral compound are not relevant and so an almost vertical ET takes place to generate the RA π.[25]

On the other hand, the C–X bond elongates in the σ isomer (*ca.* 0.14 Å for X = Br, I and *ca.* 0.23 Å for X = Cl), the C–X bond bending being very small. The RAs σ have equal C–C aromatic bond distances for the whole set of halobenzenes.

Planar RAs retain the C_{2v} symmetry of the parent neutral compound whereas C_s symmetry is present in the bended RA species.

In Fig. 2, it can be seen that for the RAs π the unpaired spin distribution and the net negative charge are mainly located on the aromatic ring with higher coefficients on the carbon atom joined to the halogen and the *para* position. For the RAs σ the unpaired spin and the negative charge are shifted to the σ C–X bond. The net spin distribution on the aromatic ring has practically disappeared.

For chlorobenzene the most stable RA is of π nature (Table 1), as expected from experimental determinations.[8,26] From inspection of the potential surface of $(C_6H_5Cl)^{\bullet -}$, a σ species with the halogen coplanar with the aromatic ring was located. This species was shown by force constants calculations to be a transition state for halogen bending. The RA σ could not be located as a minimum of the surface, in agreement to previous proposals.[8]

On the contrary, for bromobenzene the RA σ was a minimum of the potential energy surface of higher energy than the π isomer.

In the case of iodobenzene both RAs were characterized as distinct minima, but for this molecule the most stable RA is of σ nature.

Comparable results were obtained for the 2-halopyridines (X = Cl, Br, I) studied (see Table 1).

Independently of the relative stability of both isomers and assuming the system follows the Franck–Condon principle according to which electrons move faster than nuclei, we propose that once intermolecular ET to the neutral molecule occurs, the π isomer will be the first generated RA in all the cases under study.[8]

In order to reach the transition state for the IET reaction, the Franck–Condon principle is satisfied by increasing the energy of the π and σ isomers until both energy levels match each other. In the gas phase this happens by internal geometric reorganizations.

For the iodobenzene RA, the transition state for the σ–π interconversion occurs at an approximate C–I bond distance of 2.14 Å and a dihedral angle of 153°. This situation evidences that for this system, in which the C–X bond is almost coplanar with the aromatic ring in both RAs, the activation complex for the IET is reached when the σ–π symmetry is lost by deviation from planarity. Thus, an avoided crossing of potential energy surfaces[26,27,28] takes place as a result of a non-vanishing $H_{\sigma\pi}$ integral.¶ This fact results in the occurrence of the IET reaction. It should be noted that the electronic properties of the transition state are similar to that of the RA σ, the activation energy for the process being very small (*ca.* 0.2 kcal mol^{-1}).||

For bromobenzene and 2-bromopyridine RAs, we could not get a transition state for the IET reaction due to the flatness of the σ potential surface at the vicinity of the crossing point. For this RA, we propose that the avoided crossing between both surfaces (Ψ_π and Ψ_σ) occurs at an energy similar to that of the less stable σ isomer, as shown in Fig. 1, *i.e.* the difference in energy between both RAs is approximately equal to the activation energy for the IET reaction.

In the particular case of the chlorobenzene RA, we propose to take the energy difference between the RA π and the σ potential surface in the proximity of their crossing point [r(C–X) = 1.956 Å and twist angle = 148.6°] as an indication of the energy difference between both RAs. However, as the RA σ could not be located as a minimum of the surface, the IET in this system can be considered to be dissociative. The RA σ breaks while it is being formed; the C–Cl distance elongates and the C–Cl bond deviates from planarity.

RHF open shell CI calculations have been performed for the halobenzene family of compounds. The RA π is a minimum of the ground state surface (root = 1) with planar geometry. The RA σ was located on the excited potential surface (root = 3) as a planar species.

The diabatic surfaces near the crossing point were obtained by CI reaction path calculations keeping invariant the geometrical variables of the RAs π and σ (root = 1 and 3, respectively) with the C–X bond length as the reaction coordinate. The conical intersection could not be determined with this procedure.

With root = 1 and complete geometry optimization for each

---

§ Even though π and σ spatial symmetry may be lost because of C–X deviation from planarity, the orbital isomers RAs will be designated as π or σ based on their spin distribution.

¶ $H_{\sigma\pi}$ is defined by $H_{\sigma\pi} = \langle \Psi_\pi | H_{el} | \Psi_\sigma \rangle$. See references 28*a*, *b*.

|| 1 cal = 4.184 J.

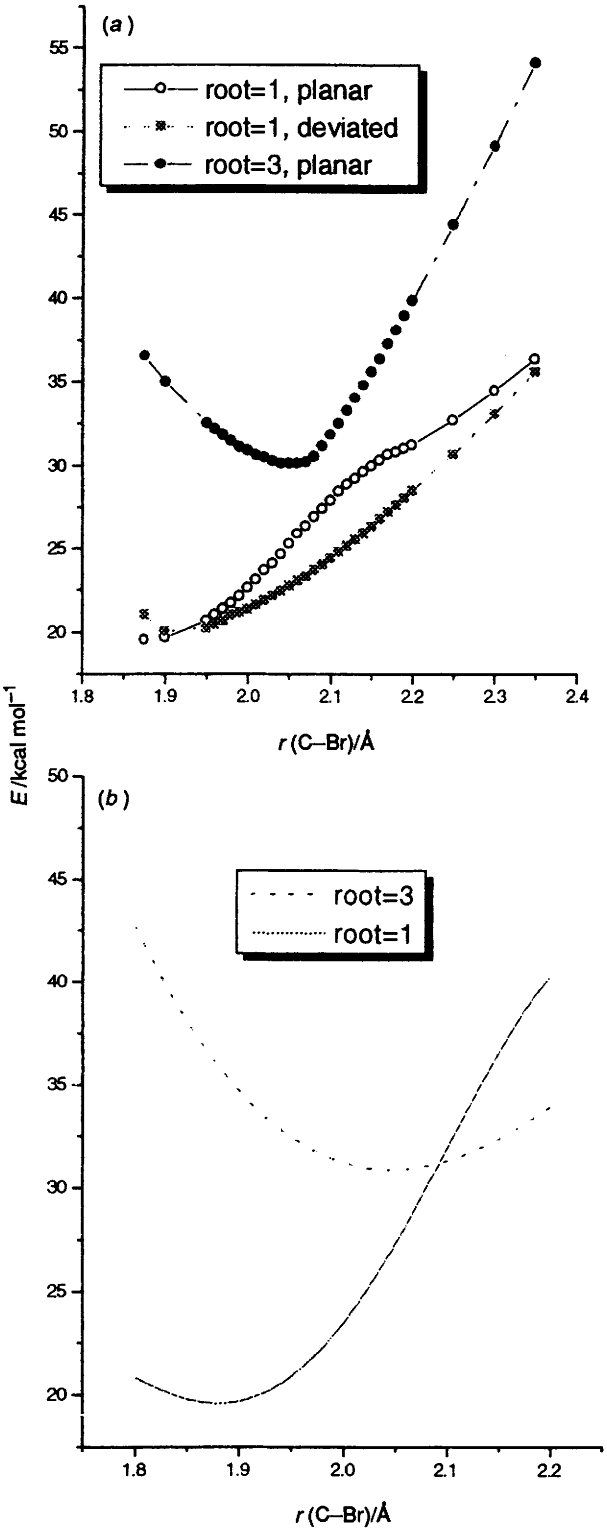

Fig. 3 (*a*) AM1 RHF/CI adiabatic surfaces for bromobenzene RA; (*b*) AM1 RHF/CI diabatic surfaces

point of the C–X bond reaction coordinate, the lower adiabatic energy path, in which deviation from planarity takes place, was determined.

The type of CI calculations and the results obtained are presented in Fig. 3 for the representative bromobenzene RA.

The CI results show similarities with the UHF ones. According to both procedures the C–X bond lengthening and bending angle are the main reaction coordinates for the minimum energy path, while the coordinates of the crossing region are practically the same. The RA σ is located on the ground state UHF surface while it is an excited species (root = 3) according to CI. The π CI surface crosses the σ one at a slightly longer C–X distance than the UHF calculation (Fig. 3).

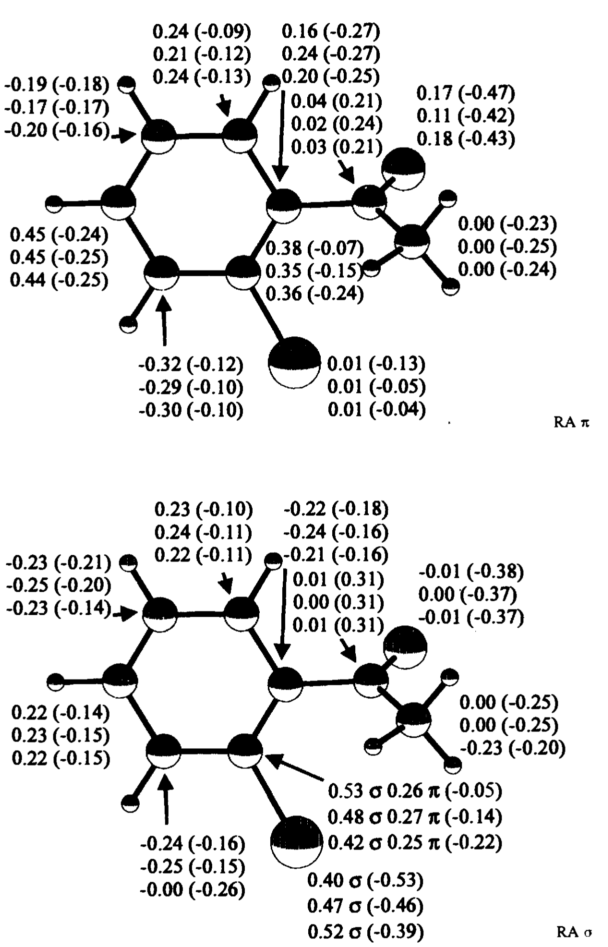

Fig. 4 Charge (in parentheses) and π unpaired spin distribution (otherwise indicated) for the *o*-haloacetophenones RA π and RA σ. From top to bottom, values for X = Cl, Br and I are shown for each atom.

Haloacetophenones and related compounds

UHF calculations have been performed for the RAs of *o*-, *m*- and *p*-haloacetophenones, *p*-bromobenzaldehyde and *p*-chlorobenzoate anion.

It was possible to localize the RA π and the RA σ as minima of the surface for all the bromo-, iodo- and chloro-substituted compounds calculated, with the exception of the RA σ of *m*-chloroacetophenone.

The most stable orbital isomers calculated for the whole set of molecules studied are of π nature.

The AM1 heats of formation of both RAs, their energy difference, as well as the most important geometric parameters are introduced in Table 2. Fragmentation rates experimentally obtained by Behar and Neta [29] and Tanner *et al.*[30] are also included.

As can be noticed, the C–X bond distance lengthening between both isomeric RAs follows the same tendency as that indicated for the halobenzenes and 2-halopyridines families of RAs. In the RAs π the C–X and C=O dihedral angles are practically coplanar with the aromatic ring except for the *ortho* substitution. In these RAs π the C–X dihedral angle deviates the most, the bigger the halogen is. In the corresponding RAs σ, the C–X bond is less bent than in the RA π, probably due to the elongation of the bond,

Table 2 AM1 parameters and experimental fragmentation rates for the RAs of haloacetophenones and related compounds

Molecule	RA	Δ_fH/kcal mol^{-1}	r(C–X)/Å	∠(C–X)/ degrees[a]	∠(C=O)/ degrees[a]	$\Delta E_{\sigma\pi}$/ kcal mol^{-1}	k_{fragm}[b]/s^{-1}	k_{fragm}[c]/s^{-1}
o-IC_6H_4COMe	π	−22.77	2.041	161.7	170.6	3.14		
	σ	−19.63	2.174	170.9	141.2			
p-IC_6H_4COMe	π	−31.34	2.021	179.4	179.9	9.72	1.4×10^5	3.5×10^9
	σ	−21.62	2.156	178.8	172.1			
m-IC_6H_4COMe	π	−29.71	2.035	179.7	179.7	9.72		1.9×10^8
	σ	−19.99	2.159	179.3	149.6			
o-BrC_6H_4COMe	π	−34.79	1.896	162.8	168.5	5.05	5.0×10^5	5.1×10^9
	σ	−29.74	2.066	161.3	173.4			
p-BrC_6H_4COMe	π	−42.42	1.878	179.9	180.0	14.13	5×10^3	3.2×10^7
	σ	−28.29	2.055	179.1	172.9			
m-BrC_6H_4COMe	π	−40.88	1.891	178.4	178.4	13.31	$\sim 10^2$	8×10^3
	σ	−27.57	2.057	178.4	167.7			
o-ClC_6H_4COMe	π	−47.20	1.728	171.6	172.7	18.25	1.5×10^3	3×10^5
	σ	−28.95	1.956	175.0	138.7			
p-ClC_6H_4COMe	π	−51.23	1.713	179.9	178.4	22.74	$\sim 10^2$	3×10^3
	σ	−28.49	1.934	179.6	158.3			
m-ClC_6H_4COMe	π	−52.09	1.727	179.7	178.8			15
	σ	—	—	—	—			
p-BrC_6H_4CHO	π	−37.42	1.878	180.0	180.0	14.33	4×10^2	
	σ	−23.09	2.050	178.1	179.6			
p-$ClC_6H_4CO_2^-$	π	−35.27	1.851	149.0	177.4	0.1	4.0×10^7	
	σ	−35.17	2.048	180.0	179.9			

[a] The dihedral angle is taken with respect to the aromatic ring; a value of 180° means coplanarity. [b] See ref. 29. [c] See ref. 30.

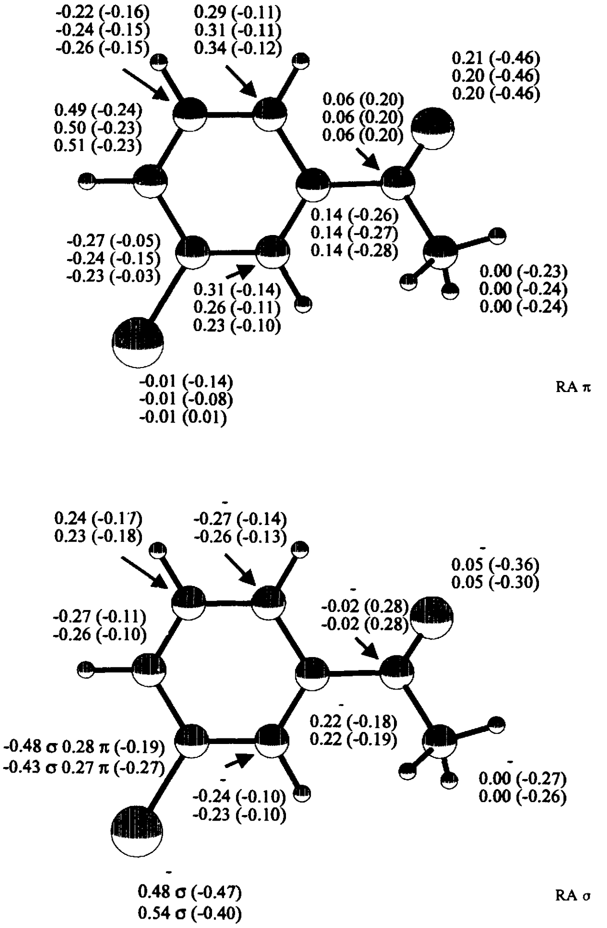

Fig. 5 Charge (in parentheses) and π unpaired spin distribution (otherwise indicated) for the *m*-haloacetophenones RA π and RA σ. From top to bottom, values for X = Cl, Br and I are shown for each atom.

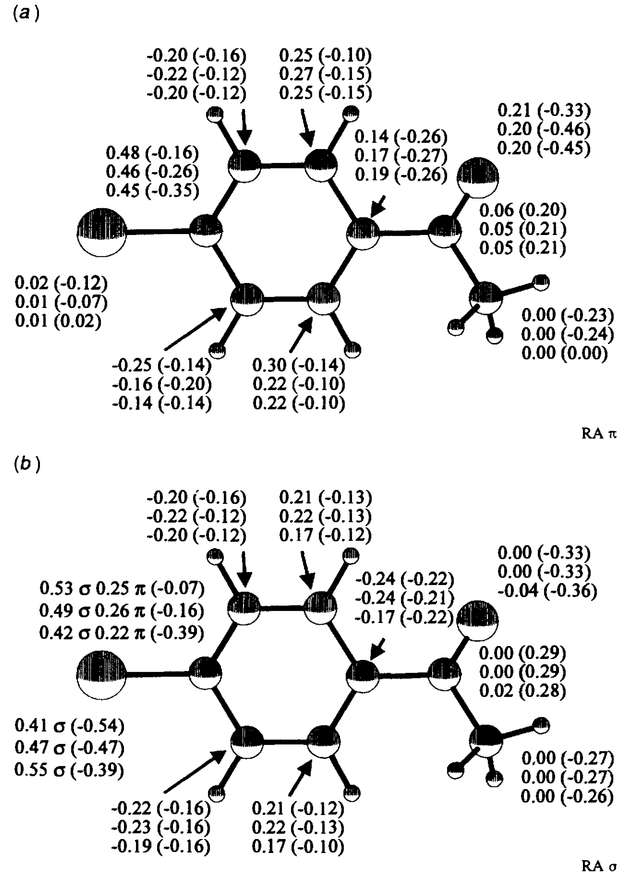

Fig. 6 Charge (in parentheses) and π unpaired spin distribution (otherwise indicated) for the *p*-haloacetophenones RA π and RA σ. From top to bottom, values for X = Cl, Br and I are shown for each atom.

whereas the C=O system increases its deviation from planarity (with the exception of the *o*-bromo-substituted derivative).

The calculated charge and spin distribution for the bromo-, iodo- and chloro-acetophenones are presented in Figs. 4–6. For the RAs π, the spin density is detected on the aromatic ring (*ca.* 70%) and the carbonyl group (*ca.* 10%), whereas the negative charge is located mainly on the oxygen atom of the carbonyl group and on the aromatic ring. For the RAs σ the spin

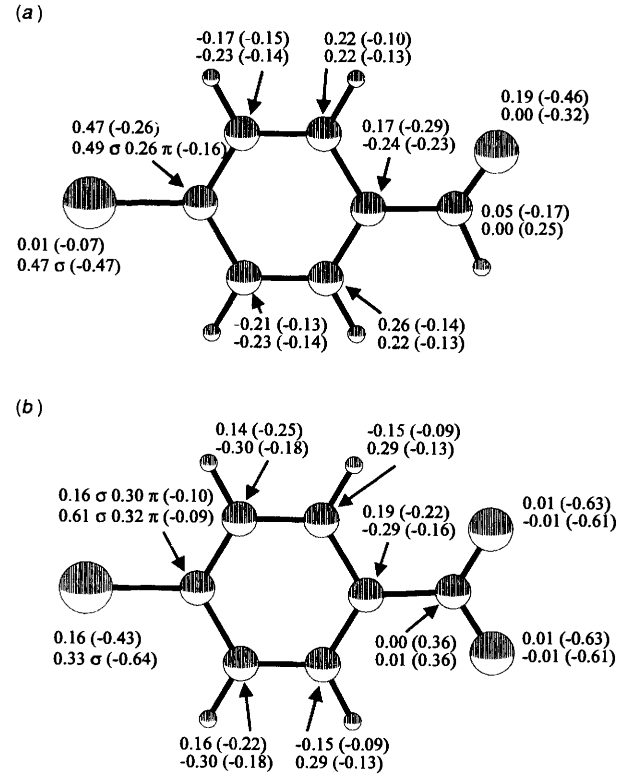

Fig. 7 Charge (in parentheses) and π unpaired spin distribution (otherwise indicated) for *p*-bromobenzaldehyde (*a*) and *p*-bromobenzoate (*b*) RAs. From top to bottom, values for RA π and RA σ are shown for each atom.

distribution is shifted toward the C–X bond and the negative charge moves mainly from the aromatic ring to the halogen.

There are no significant differences between the *p*-haloacetophenones and *p*-bromobenzaldehyde spin and charge localization, as can be seen in Fig. 7(*a*).

The charge and spin distribution for the RA of *p*-chlorobenzoate anion are shown in Fig. 7(*b*).

This radical dianion shows a greater degree of σ spin and charge distribution at the C–X bond of the RA π, which can be explained by a σ–π overlap due to the C–X bending. The CO_2^- group does not show spin delocalization, but negative charge. The RA σ has the extra electron strongly restricted to the C–X system (94%) and the negative charge on the aromatic ring and the carboxylate group. Because of repulsion, generation of a radical dianion represents an energetically unfavourable process.

Halobenzonitriles

Table 3 shows the AM1 determinations of the orbital isomers for RAs of halobenzonitrile derivatives. Fragmentation rates experimentally obtained in aqueous solution by Neta and Behar[31] are also included for some chloro- and bromo-compounds.

Discussion

The dissociation of these RAs in the sense indicated by eqn. (1) is calculated as an endergonic process in the gas phase, however it is expected to be an exergonic reaction mainly in solution due to the solvation stabilization of the anionic species generated, as demonstrated by the aqueous phase calculation.[32] By including this solvent effect, the IET reaction (orbital isomerism) could be considered the rate-limiting step for the fragmentation process.

In the present calculations, with the exception of iodobenzene, it was not possible to locate the transition state for the reaction. The flatness of the σ potential surface, of higher energy than the π one, near the crossing point led us to assume the difference $\Delta E_{\sigma\pi}$ as indicative of the $\Delta G^{\ddagger}$ for the IET step.

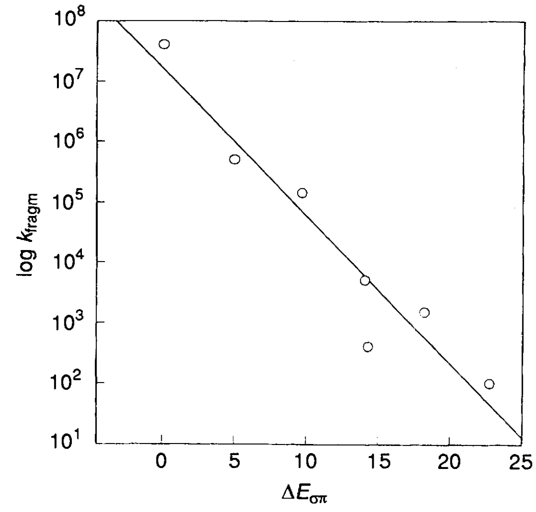

Fig. 8 Correlation between the $k_{\text{fragm}}/\text{s}^{-1}$ and $\Delta E_{\sigma\pi}/\text{kcal mol}^{-1}$ for haloacetophenones and related compounds. Rates measured in aqueous solution.

According to the Marcus theory for outer-sphere ET,[33] the $\Delta G^{\ddagger}$ depends on the corrected standard free energy change $\Delta G^{0'}$ and on the reorganization energy λ [eqn. (2)].

$$\Delta G^{\ddagger} \approx \frac{\lambda}{4}\left(1 + \frac{\Delta G^{0'}}{\lambda}\right)^2 \qquad (2)$$

Considering the IET reaction for the RAs under study within the framework of the Marcus theory, a linear plot of $\Delta G^{\ddagger}$ *vs.* $\Delta G^{0'}$ could be expected for a limited set of $\Delta G^{0'}$ values whenever λ is approximately constant for each family under study.** On this basis the calculated energy difference between both RAs could be assumed to correlate with their experimentally determined scission rate k_{fragm} even when the $\Delta E_{\sigma\pi}$ is not corrected on account of the relative positions and nature of the substituents, *i.e.* the 'effective IET distance' is not taken into consideration.[33]

$\Delta E_{\sigma\pi}$ is also expected to be modified in solution owing to the stabilization of the σ species. However, this stabilization can be thought to be similar for a given family of RAs σ, resulting in a relative order of the $\Delta E_{\sigma\pi}$ in solution closer to the ones obtained for the gas phase.

Energy differences for halobenzenes and 2-halopyridines (Table 1) indicate that the fragmentation reaction rate follows the order: Cl < Br < I as is known from experimental determinations for other haloaromatic compounds.[34] For halobenzenes, the fragmentation rate has been shown to be diffusional,[2c,35] while AM1 seems to overestimate their activation barriers.

A good correlation ($r^2 \approx 0.956$) has been achieved for the *o*- and *p*-haloacetophenone series of compounds between the AM1 calculated difference in heats of formation of both orbital isomers, and the experimentally determined fragmentation rate in aqueous solution (Fig. 8 and Table 2). The *meta*-substituted compounds depart from the line at a constant value.

More recently, new experimental data of fragmentation rates

** The considered set of $\Delta G^{0'}$ should differ sufficiently from $-\lambda$. See ref. 1.

Table 3 AM1 parameters and experimental fragmentation rates for the RAs of halobenzonitriles

Molecule	RA	Δ_fH/ kcal mol^{-1}	r(C–X)/Å	∠(C–X)/ degrees^a	∠(C≡N)/ degrees^a	$\Delta E_{\sigma\pi}$/ kcal mol^{-1}	$k_{\text{fragm}}{}^b$/ s^{-1}
o-IC_6H_4CN	π	40.71	2.025	176.1	175.7	5.45	
	σ	46.16	2.155	177.9	177.0		
p-IC_6H_4CN	π	37.47	2.022	172.5	179.6	6.88	
	σ	44.35	2.155	179.0	179.3		
m-IC_6H_4CN	π	39.15	2.029	180.0	173.6	6.01	
	σ	45.16	2.158	180.0	176.0		
o-BrC_6H_4CN	π	29.40	1.882	176.6	178.4	9.82	
	σ	39.22	2.048	177.8	177.4		
p-BrC_6H_4CN	π	26.45	1.876	174.7	176.5	11.21	$>3 \times 10^7$
	σ	37.66	2.052	178.9	179.4		
m-BrC_6H_4CN	π	28.19	1.889	179.2	166.6	10.41	8×10^6
	σ	38.60	2.058	180.0	176.0		
o-ClC_6H_4CN	π	18.60	1.720	180.0	167.1	18.98	9×10^6
	σ	37.58	1.938	177.8	175.7		
p-ClC_6H_4CN	π	16.26	1.715	179.5	130.3	19.71	5×10^6
	σ	35.97	1.954	179.2	178.7		
m-ClC_6H_4CN	π	17.30	1.729	179.7	164.6	19.71	4.2×10^4
	σ	37.01	1.948	180.0	176.0		

^{a} The twist angle is taken with respect to the aromatic ring; a value of 180° means coplanarity. ^{b} See ref. 31.

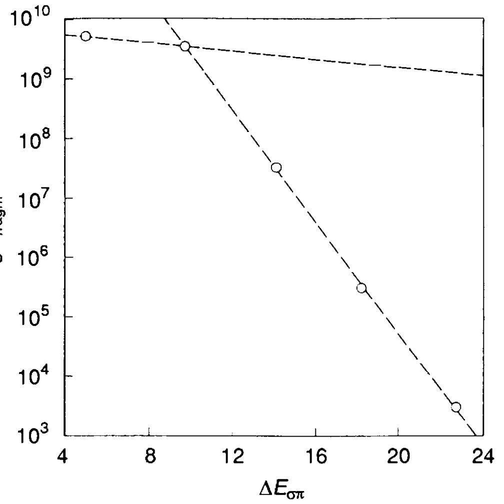

Fig. 9 Correlation between the k_{fragm}/s^{-1} and $\Delta E_{\sigma\pi}$/kcal mol^{-1} for haloacetophenones and related compounds. Rates measured in acetonitrile.

of haloacetophenones RAs has appeared[30] using acetonitrile as solvent. Even better linear correlation between k_{fragm} and $\Delta E_{\sigma\pi}$ was obtained in this case as depicted in Fig. 9.

A good linear behaviour is observed ($r^2 = 0.999$) for this set of compounds when the cleavage rates are smaller than 1×10^9 s^{-1}, whereas smoothness is observed for diffusional rates.

For the halobenzonitrile family, and even though all the pairs of RAs were attained, good correlation ($r^2 = 0.969$) was obtained just for those compounds whose fragmentation rates were available (o-, p-chlorobenzonitrile and p-bromobenzonitrile).

The present calculations agree with the fragmentation rate order I > Br > Cl and for a particular halogen with the order *ortho* > *para*. *Meta-* and *para*-substitution are predicted to have similar fragmentation rates while the experimental order is *meta* ≪ *para*.

On a thermodynamic basis and for the same halogen, the *ortho*- and *para*-substituted RAs σ are expected to have almost the same heat of formation, since the extra electron is mainly localized in a separate C–X system as shown by our calculations. By contrast in the *ortho*-substituted RA π, the steric effect is accompanied by a loss of planarity that leads to a greater destabilization with regard to the *para*-substituted RA π. This effect depends on the size of the halogen as discussed above. These factors result in *ortho*-$\Delta E_{\sigma\pi}$ < *para*-$\Delta E_{\sigma\pi}$.

This positional order can also be explained[31] in terms of spin distribution. From our calculations it can be seen that there is an important unpaired spin distribution at the carbon of the C–X bond for the RA π of the *ortho* and *para* compounds, this distribution being higher for the *para* compound. On the other hand, the total spin distribution in the vicinity of the C–X bond is higher for the *ortho* ones, which could increase the probability of the IET to this bond.

According to our AM1 UHF calculations, the thermodynamic and kinetic effects work together for the *ortho* and *para* RAs as expected from Marcus theory.

As indicated in Figs. 3–5, the RA π of the *meta*-substituted compounds has a lesser spin density at the carbon and halogen atoms of the C–X bond, which could explain their low cleavage rates. However, the calculated energy differences between both isomers do not correlate with the experimental behaviour, but they are quite similar to the differences calculated for the *para* compounds. This similarity could indicate that either the $\Delta E_{\sigma\pi}$ for the *meta* family is not well predicted or that the IET reaction takes place in this family with a different reorganization energy λ. Nevertheless, this last possibility would mean an unexpected extremely high *meta* λ value compared with the corresponding λ value for the *ortho* and *para* compounds.

Conclusions

IET in haloaromatic compounds can be viewed as the interconversion of RA π and RA σ.

The most stable RAs are generally of π nature, in accordance with the orbital symmetry of the lowest unoccupied molecular orbitals (LUMOs) of their parent neutral molecule. For iodobenzene and 2-iodopyridine the RA σ is the most stable one, even though their LUMOs are of π symmetry.

The C–X bond elongation and its dihedral bending angle are the most relevant coordinates for the IET reaction. This loss of symmetry near the crossing point of the π and σ potential surfaces is a decisive factor for the reaction, mainly in those cases where the RA π and the RA σ retain their spatial symmetry.

The activation energy for the reaction depends on the energy difference between the π and σ RAs according to the Marcus equation. The IET is proposed to be the rate-determining step for the cleavage reactions of haloaromatic RAs. Very good correlations were obtained between fragmentation rates and calculated $\Delta E_{\sigma\pi}$ values. This is presented for haloacetophenones RAs in aqueous solution and acetonitrile, the latter being the best available correlation set. In addition, a good relationship for some halobenzonitrile RAs in aqueous solution was also obtained.

Prediction of theoretical cleavage rates that cannot be afforded by experiments could be drawn on the basis of the proposed relationship.

The AM1 UHF correlation obtained indicates the validity of the procedure to study the IET reaction of haloaromatic compounds, despite the results previously reported in the study of halide compounds.[36]

Acknowledgements

This work was supported in part by the *Consejo Nacional de Investigaciones Científicas y Técnicas* (CONICET), the *Consejo de Investigaciones de la Provincia de Córdoba* (CONICOR) and *Fundación Antorchas*. J. S. D. gratefully acknowledges receipt of a fellowship from CONICET. INFIQC is jointly sponsored by CONICET and the *Universidad Nacional de Córdoba*.

References

1 L. Eberson, *Electron Transfer Reactions in Organic Chemistry*, Springer-Verlag, New York, 1987.

2 (*a*) R. A. Rossi and R. H. de Rossi, *Aromatic Substitution by the* $S_{RN}1$ *Mechanism*, ACS Monograph 178, American Chemical Society, Washington DC, 1983; (*b*) W. R. Bowman, *Chem. Soc. Rev.*, 1988, **17**, 283; (*c*) J. M. Savéant, *Adv. Phys. Org. Chem.*, 1990, **26**, 1; (*d*) R. K. Norris, *Comprehensive Organic Synthesis*, eds. B. M. Trost and I. Fleming, Pergamon, New York, 1991, vol. 4, p. 451.

3 (*a*) E. M. Arnett and R. A. Flowers, II, *Chem. Soc. Rev.*, 1993, **22**, 9; (*b*) X.-M. Zhang, *J. Chem. Soc., Perkin Trans. 2*, 1993, 2275; (*c*) K. Daasbjerg, *J. Chem. Soc., Perkin Trans. 2*, 1994, 1275.

4 T. Clark, *J. Am. Chem. Soc.*, 1988, **110**, 1672.

5 Strained aliphatic RAs are theoretically predicted to exist. See for instance: A. B. Pierini, A. N. Santiago and R. A. Rossi, *Tetrahedron*, 1991, **47**, 941.

6 R. A. Rossi, A. B. Pierini and S. M. Palacios, *Advances in Free Radical Chemistry*, ed. D. D. Tanner, Greenwich, vol. 1, 1990; (*b*) R. A. Rossi and A. N. Santiago, *Trends in Organic Chemistry*, 1992, **3**, 193.

7 (*a*) M. J. S. Dewar and K. Narayanaswami, *J. Am. Chem. Soc.*, 1964, **86**, 2422; (*b*) M. J. S. Dewar, A. H. Pakiari and A. B. Pierini, *J. Am. Chem. Soc.*, 1982, **104**, 3242.

8 D. D. Clarke and C. A. Coulson, *J. Chem. Soc. A*, 1969, 169.

9 (*a*) B. Bigot, D. Roux and L. Salem, *J. Am. Chem. Soc.*, 1981, **103**, 5271; (*b*) T. Clark, *Faraday Discuss. Chem. Soc.*, 1984, **78**, 203; (*c*) M. Hotokka, B. O. Roos and L. Eberson, *J. Chem. Soc., Perkin Trans. 2*, 1979, 1986.

10 (*a*) M. C. R. Symons, *J. Chem. Soc., Chem. Commun.*, 1977, 408; (*b*) M. C. R. Symons, *J. Chem. Soc., Faraday Trans. 1*, 1981, **77**, 783; (*c*) M. C. R. Symons and W. R. Bowman, *J. Chem. Soc., Perkin Trans. 2*, 1990, 975.

11 (*a*) H. Villar, E. A. Castro and R. A. Rossi, *Can. J. Chem.*, 1982, **60**, 2525; (*b*) M. C. R. Symons, *Pure Appl. Chem.*, 1981, **53**, 223; (*c*) H. Villar, E. A. Castro and R. A. Rossi, *Z. Naturforsch., Teil A*, 1984, **39**, 49.

12 (*a*) A. Kuki, *Structure and Bonding*, Springer-Verlag, Berlin, 1991, p. 50; (*b*) R. A. Marcus and N. Sutin, *Biochim. Biophys. Acta*, 1985, **811**, 265; (*c*) M. Braga, A. Broo and S. Larsson, *Chem. Phys.*, 1991, **156**, 1; (*d*) M. Braga and S. Larsson, *Chem. Phys. Lett.*, 1993, **213**, 217; (*e*) M. N. Paddon-Row, *Acc. Chem. Res.*, 1994, **27**, 18; (*f*) M. D. Newton, *Chem. Rev.*, 1991, **91**, 767.

13 (*a*) B. M. Hoffman, M. J. Natan, J. M. Nocek and S. A. Wallin, *Structure and Bonding*, Springer-Verlag, Berlin, 1991, p. 86; (*b*) S. S. Isied, M. Y. Ogawa and J. F. Wishart, *Chem. Rev.*, 1992, **92**, 381; (*c*) D. N. Beratan, J. N. Betts and J. N. Onuchic, *Science*, 1991, **252**, 1285; (*d*) J. N. Betts, D. N. Beratan and J. N. Onuchic, *J. Am. Chem. Soc.*, 1992, **114**, 4043.

14 D. N. Beratan, *Mol. Cryst. Liq. Cryst.*, 1990, **190**, 85.

15 (*a*) J. Casado, I. Gallardo and M. Moreno, *J. Electroanal. Chem.*, 1987, **219**, 197; (*b*) A. B. Pierini, J. S. Duca, Jr. and M. T. Baumgartner, *J. Mol. Struct. (Theochem.)*, 1994, **311**, 343.

16 M. Chanon, M. Rajzmann and F. Chanon, *Tetrahedron*, 1990, **46**, 6193.

17 C. P. Andrieux, J. M. Savéant and D. Zann, *Nouv. J. Chim.*, 1984, **8**, 107.

18 C. Glidewell, *Chem. Scr.*, 1985, **25**, 142.

19 (*a*) X. Martin, J. Marquet and J. M. Lluch, *J. Chem. Soc., Perkin Trans. 2*, 1993, 87; (*b*) M.-S. Tsai, M.-C. Ou and S.-Y. Chu, *J. Mol. Struct. (Theochem.)*, 1994, **311**, 169.

20 M. C. Lazana, M. L. Franco and B. J. Herold, *J. Am. Chem. Soc.*, 1989, **111**, 8640.

21 M. J. S. Dewar, E. G. Zoebisch, E. F. Healy and J. J. Stewart, *J. Am. Chem. Soc.*, 1985, **107**, 3902.

22 D. A. Liotard, E. F. Healy, J. M. Ruiz and M. J. S. Dewar, AMPAC version 2.1, *Quantum Chemistry Program Exchange*, program 506, *QCPE Bull.*, 1989, **9**, 123.

23 J. A. Pople and R. K. Nesbet, *J. Chem. Phys.*, 1954, **22**, 571.

24 (*a*) J. W. McIver and A. Komornicki, *Chem. Phys. Lett.*, 1971, **10**, 303; (*b*) J. W. McIver and A. Komornicki, *J. Am. Chem. Soc.*, 1972, **94**, 2625.

25 G. F. Pedulli, *Res. Chem. Intermed.*, 1993, **19**, 617.

26 R. Dressler, M. Allan and E. Haselbach, *Chimia*, 1985, **39**, 385.

27 L. Salem, *Electrons in Chemical Reactions: First Principles*, Wiley, New York, 1982.

28 (*a*) M. D. Todd, K. V. Mikkelsen, J. T. Hupp and M. A. Ratner, *New J. Chem.*, 1991, **15**, 97; (*b*) G. J. Kavarnos and N. J. Turro, *Chem. Rev.*, 1986, **86**, 401.

29 D. Behar and P. Neta, *J. Am. Chem. Soc.*, 1981, **103**, 2280.

30 D. D. Tanner, J. J. Chen, L. Chen and C. Luelo, *J. Am. Chem. Soc.*, 1991, **113**, 8074.

31 P. Neta and D. Behar, *J. Am. Chem. Soc.*, 1981, **103**, 103.

32 A. B. Pierini and J. S. Duca, Jr., unpublished results with AMPAC 5.0, © 1994 Semichem., 7128 Summit, Shawnee, KS 66216.

33 R. A. Marcus, *Angew. Chem., Int. Ed. Engl.*, 1993, **32**, 1111 and references cited therein.

34 M. Meot-Ner, P. Neta, R. K. Norris and K. Wilson, *J. Phys. Chem.*, 1986, **90**, 168.

35 F. M'Halla, J. Pinson and J. M. Savéant, *J. Am. Chem. Soc.*, 1980, **102**, 4120.

36 M. J. S. Dewar and E. G. Zoebisch, *J. Mol. Struct. (Theochem.)*, 1988, **180**, 1.

Paper 4/07437H
Received 6th December 1994
Accepted 6th April 1995